Trion, biexciton, and exciton dynamics in single self-assembled CdSe quantum dots

B. Patton, W. Langbein, and U. Woggon*
Experimentelle Physik IIb, Universität Dortmund, Otto-Hahn-Str. 4, 44221 Dortmund, Germany
(Received 7 February 2003; published 18 September 2003)

We present an analysis of time- and polarization-resolved data taken in microphotoluminescence experiments on individual CdSe/ZnSe quantum dots grown by molecular beam epitaxy. The identification of individual dots was performed by a spectral jitter correlation technique and by their polarization properties and density dependences. Decay times are given for exciton, trion, and biexciton states and evidence is shown for a spin-relaxation-limited energy relaxation of the trion. For the bright-exciton state the temperature dependence of the decay time is studied and a repopulation from the dark-exciton state is observed. Trion binding energies of 15–22 meV and biexciton binding energies of 19–26 meV are found.

DOI: 10.1103/PhysRevB.68.125316 PACS number(s): 78.67.Hc, 78.55.Et, 78.66.Hf

I. INTRODUCTION

The original interest in self-assembled wide-gap semiconductor nanostructures was driven by their potential applications in light-emitting or lasing devices for the green, blue, or ultraviolet spectral ranges.[1–4] Nowadays, a further peculiarity attracts attention to wide-gap materials: Coulomb correlation energies have been observed in quantum dots which are up to 10 times higher than those in III-V semiconductor materials.[5–9] It makes, e.g., II-VI semiconductor quantum dots interesting candidates in the study of few-particle states such as trions, biexcitons, or charged biexcitons, yielding binding energies, lifetimes, and fine structure of these electron-hole complexes with both integer and half-integer total spin states.

Much of the initial work on the optical properties of self-assembled II-VI quantum dots has focused on ensembles of dots.[10–14] The spectroscopy of such groups exhibits an inhomogeneous broadening of spectral features due to variance in the geometry and composition of different dots within the same sample. More recent times have seen the publication of data on single CdSe/ZnSe quantum dots.[6–8,15–20] An advantage of performing measurements on individual dots is that the homogeneous broadening for different transitions in the dots should be accessible. However, when single-dot spectroscopy was initially attempted it was found that the spectral position of optical transitions in the dot varied with time. This spectral jitter reflects the effect of fluctuating electrostatic fields on the energy levels within the dot.[21–25] The mechanism which generates the fields is the trapping of charge carriers in the vicinity of individual dots leading to a local electric field and a resulting Stark shift in the position of spectral features corresponding to that dot. The magnitude and dynamics of the shift due to this quantum confined Stark effect differ between different dots, since they are located at different positions. By correlating the dynamic shift in the spectral position of several emission peaks one is therefore able to identify emission peaks from transitions within the same dot.

In this paper we present measurements on self-assembled CdSe quantum dots whence we perform a correlation analysis on the spectral jitter which allows us to group spectral transitions from individual dots. With this information we are able to label individual spectral features according to the quasiparticles which generate them. In doing so we have focused on properties of excitons with an additional charge (trions), a quasiparticle in which a single electron (hole) interacts with a spin-singlet state of two holes (electrons), respectively.

The trion is an interesting elementary excitation because its radiative decay can be used to monitor properties of single electrons or holes which are usually optically inaccessible. It is expected that the number of charge carriers within a quantum dot will affect both the lifetime of the state and its other spectroscopic properties such as exchange splitting and binding energy. The existence of trions was first reported almost ten years ago[26–28] and predominantly studied in quantum well structures (see, e.g., Ref. 29–31 and references therein). Only recently were trion states studied in self-assembled quantum dots using magnetophotoluminescence and microphotoluminescence (μPL) experiments.[32–39] In parallel the problem of charged nanocrystals has been addressed through experiments on colloidal CdSe quantum dots.[40] While detailed theoretical work predicts binding and charging energies,[41–44] there is a substantial lack of experimental data with which to be compared.

In the work presented here, we have measured the binding energies of trions and biexcitons relative to the exciton. We give a systematic study of both the fine structure and the dynamics of all three quasiparticles. The observed energy shift of the trion transition due to the presence of an additional charge carrier is compared with data obtained for colloidal CdSe dots[40] and those predicted in theory.[41] We also give data on the lifetimes of trion states and show evidence for a spin-relaxation-limited energy relaxation of the trion. Finally, we present a temperature-dependent study of the bright-exciton decay and discuss the influence of a thermally activated repopulation from the dark-exciton state.

II. EXPERIMENT

The results presented in this paper were obtained from a sample containing CdSe quantum dots embedded in ZnSe. Previous work has characterized such systems.[5,13] The sample consists of three monolayers of CdSe grown between ZnSe layers of 25 and 50 nm thickness. In Ref. 5 we found

that the dots consist of Cd-rich regions embedded in a ZnCdSe matrix. The strong interdiffusion of Cd within ZnSe leads to islands with concentrations of Cd greater than 70% forming within a ZnCdSe quantum well. It is these islands that trap the charge carriers, forming the quantum dots (QD's).

To enable small numbers of dots to be isolated the sample was etched into an array of mesa structures (for details see Ref. 45). The separation between each mesa was chosen to be 200 μm to allow us to isolate individual mesas both when exciting the sample and when collecting the photoluminescence. The mesas are patterned in a square geometry and vary in size from $(1\ \mu\mathrm{m})^2$ down to $(50\ \mathrm{nm})^2$, meaning that, at the lower end of this range, only a few (<5) optically active dots would be expected to be in each mesa.

All the data presented here were detected in a μPL geometry with the sample mounted in a cold-finger cryostat, allowing measurement down to a sample temperature of 10 K. Unless otherwise stated, all the data was taken at a temperature of 13 K. The excitation source was a frequency-doubled, mode-locked Ti-sapphire laser working in the range of 400–440 nm. When an excitation intensity is presented it is given with respect to a reference intensity $I_0=250\ \mu$W focused into a 50-μm-diam excitation spot. The photoluminescence was collected with a 0.4-NA-long working distance objective lens. Subsequently, the time-resolved data were collected by a streak camera with a 4-ps resolution, and the time-integrated, polarization-resolved data come from either a 0.5-m or a 2-m spectrometer, with each of which using their own nitrogen-cooled charge-coupled device array.

As discussed above, the trapping of carriers in the nanoenvirons of these dots will lead to changes in the position of spectral features over time. An example of this is given in the jitter spectrum in Fig. 1 which was generated by taking 256 consecutive spectra of 1 s integration time. This change in the emission energy of the spectral features is readily discernible. However, it should also be noted that the rate of change of the field is sufficiently slow that the dot may go through repeated exciton creation and decay cycles before a resolvable change in the magnitude of the shift becomes apparent. This means that even though certain spectral features (such as trions and excitons) cannot be present simultaneously, the slow rate of change of the Stark shift compared to the time scale of the population dynamics and the change in the charge state in the dots sees them appearing in the same spectra. Hence, we can make a correlation of the form

$$C_{ij}=\frac{\langle E_iE_j\rangle-\langle E_i\rangle\langle E_j\rangle}{\sigma_i\sigma_j}, \tag{1}$$

with E_i being the time-dependent position of peak number i, $\langle\cdots\rangle$ denotes the time average and $\sigma_i=\sqrt{\langle E_i^2\rangle-\langle E_i\rangle^2}$ is the standard deviation of E_i. This correlation coefficient will be exactly unity for peaks that show up to a scaling factor the same time evolution, and we expect peaks with a high correlation coefficient to come from the same dot.

More specifically, the spectral position of each transition can be expanded in powers of the local electric field at the position of the corresponding QD k $\mathbf{F}_k$:

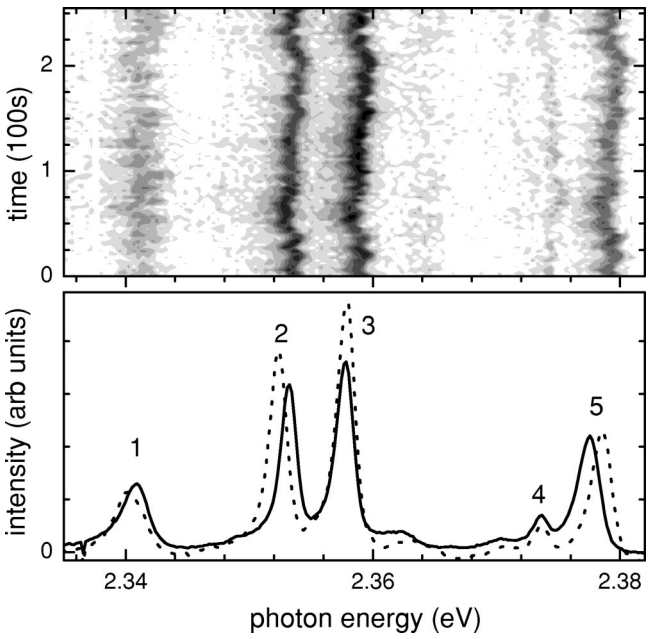

FIG. 1. Top: spectrally resolved intensity vs time (logarithmic greyscale). Bottom: jitter-corrected time-integrated photoluminescence spectra for the two linear polarizations along [110] and $[1\bar{1}0]$. Peaks are marked by their index in the correlation matrix given in the text.

$$E_i=E_{i0}+\mathbf{p}_i\mathbf{F}_k+\frac{1}{2}\mathbf{F}_kP_i\mathbf{F}_k+O(\mathbf{F}^3), \tag{2}$$

with the permanent dipole moment $\mathbf{p}_i=p_i\hat{p}_i$ of amplitude p_i and direction $\hat{p}_i$, and the polarizability tensor P_i of the transition. Using only the linear term and assuming zero average field $\langle\mathbf{F}\rangle=0$ (can be satisfied by the choice of E_{i0}), we find

$$C_{ij}=\frac{\langle(\hat{p}_i\mathbf{F}_k)(\hat{p}_j\mathbf{F}_l)\rangle}{\sqrt{\langle(\hat{p}_i\mathbf{F}_k)^2\rangle\langle(\hat{p}_j\mathbf{F}_l)^2\rangle}}. \tag{3}$$

The correlation is thus independent of the amplitude p_i, which is only a scaling factor of the fluctuations. For transitions in the same dot ($k=l$), the correlation is unity for parallel dipole moments ($\hat{p}_i=\hat{p}_j$). In other cases, the correlation depends on the directional distribution of $\mathbf{F}$. For transitions in different dots, the correlation depends also on the correlation between the fields $\mathbf{F}_k$ and $\mathbf{F}_l$. If they are uncorrelated ($\langle\mathbf{F}_k\mathbf{F}_l\rangle=0$), C_{ij} will vanish. Otherwise a finite value can be present. Since the investigated transitions are all located within the size of the investigated mesa, the fields are likely to be partly correlated, and thus even transitions of different dots can show some correlation.

To make the jitter correlation described in Eq. (1) we take a series of consecutive spectra with each individual spectrum having an integration time of approximately 1 s (naturally, this depends on the intensity of an individual mesa). We then do a simple peak-finding routine to find the position of each transition for each spectrum. We can now correlate the change in spectral position for each transition, allowing us to group spectral features together. Due to the statistical nature

of the shift, the correlation value is subject to error for a finite ensemble of emission energies in time. Additionally, due to the finite accuracy of the peak position, even fully correlated peak shifts would show a measured correlation smaller than unity. Taking this into account, about ten mesas each containing one to three dots have been screened to extract reliable data.

The correlation coefficients found for an individual mesa were always arranged in two groups, one in the range -0.2–0.2, which we assigned to transitions of different dots, and another one in the range 0.7–1.0, which we assigned to transitions in the same dot. The advantage of this method is that it allows us to rapidly find interesting groups of lines within spectra that would otherwise be laborious to work with.

III. RESULTS AND DISCUSSION

A. Peak assignment, fine structure, and binding energies

Having identified transitions as being correlated, we may examine other properties of their emission to identify their source. To illustrate the identification of features we take the correlated peaks in Fig. 1 as an example. This figure shows a typical time-integrated photoluminescence spectrum for which five peaks have been identified in order to perform a jitter correlation. The resulting correlation matrix for these peaks is

$$C_{ij}=\begin{vmatrix} 1 & -0.143 & -0.138 & -0.173 & -0.108 \\ \ldots & 1 & 0.915 & -0.113 & 0.907 \\ \ldots & \ldots & 1 & -0.145 & 0.882 \\ \ldots & \ldots & \ldots & 1 & -0.130 \\ \ldots & \ldots & \ldots & \ldots & 1 \end{vmatrix}.$$

Since the matrix is symmetric, we present only the upper half. It can be seen that peaks 2, 3, and 5 are correlated while peaks 1 and 4 belong to different dots. To identify the transitions further we use the fact that exchange interaction in quantum dots will lead to a polarization splitting of the two spin-degenerate optically active exciton states into a doublet of orthogonal linear polarizations (a detailed discussion of the observed fine structure effects will be given below). Exchange interaction is also responsible for the fact that biexcitons and excitons show an interesting effect; for one polarization the peak for the biexciton transition is at a lower energy than for the other polarization while the excitonic peak is at a higher energy. This process whereby the peaks for one polarization act as bookends to those of the other polarization is characteristic of a biexciton and exciton within a single dot and hence allows us to identify peaks 2 and 5 as being such a pair. Trions will exhibit no splitting and it can be seen that this is the case for peak 3.

Exciton, biexciton, and trion PL peaks were then further examined with respect to their excitation density dependences. An example of the excitation-density-dependent response of the dots is given in Fig. 2 which shows the time-integrated photoluminescence of a single mesa at multiple excitation intensities. In accordance with the above discussion it can be seen that the trion and exciton are present at the lowest excitation intensities and the biexciton is absent. With increasing excitation the emission from the exciton is seen to saturate and emission from the biexciton is observed. The exciton is always identified as being the peak present at low excitation energies.

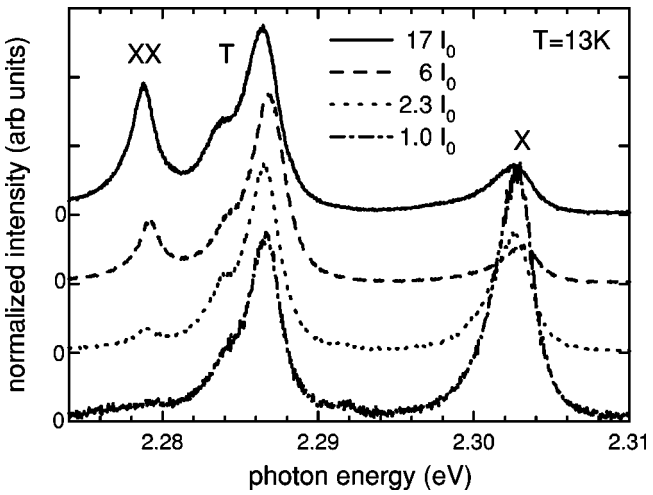

FIG. 2. Time-integrated photoluminescence of single mesa at multiple excitation intensities. All spectra have been normalized to the peak at 2.287 eV and are vertically displaced for clarity. $I_0 = 250\ \mu$W.

Figure 3 shows the binding energies we derived using this method for trions and biexcitons plotted versus their emission energy.[46] As a result of this analysis we have found biexciton binding energies of 19–26 meV and trion binding energies of 15–22 meV. We have always observed the trion emission at a higher energy than that of the corresponding biexciton. Note that the binding energy for both quasiparticles is quite well defined. Interestingly, the trion binding energy is comparable to energy shifts observed in charged colloidal CdSe nanocrystals.[40] Theoretical predictions[41] indicate that singly charged nanocrystals should emit 22 meV to the red of the neutral exciton emission. For the biexciton binding energy the data reproduce well the value measured in quantum dot ensembles by use of femtosecond four-wave mixing (FWM) and two-photon absorption techniques.[5] No systematic trend of biexciton binding energies with increasing exciton localization is observed. This may be due to the 150-meV energy window in which we detected biexciton emission being too small to observe any pronounced confinement induced increase in biexciton binding energy.

Next we discuss the observed polarization splittings (lower part of Fig. 3) which have been inferred from the peak fine structure observed when detecting the photoluminescence polarized along the $[110]$ and $[1\bar{1}0]$ crystal directions. The fine structure is due to exchange interaction which has been treated theoretically, e.g., in Refs. 47–50 and observed in both semiconductor nanocrystals[51–53] and epitaxially grown III-V (Ref. 37 and 54) and II-VI (Refs. 55,56 and 58) quantum dots. Electron-hole exchange interaction splits the fourfold-degenerate heavy-hole exciton state by a splitting energy δ_0 into a radiative doublet with total pair angular

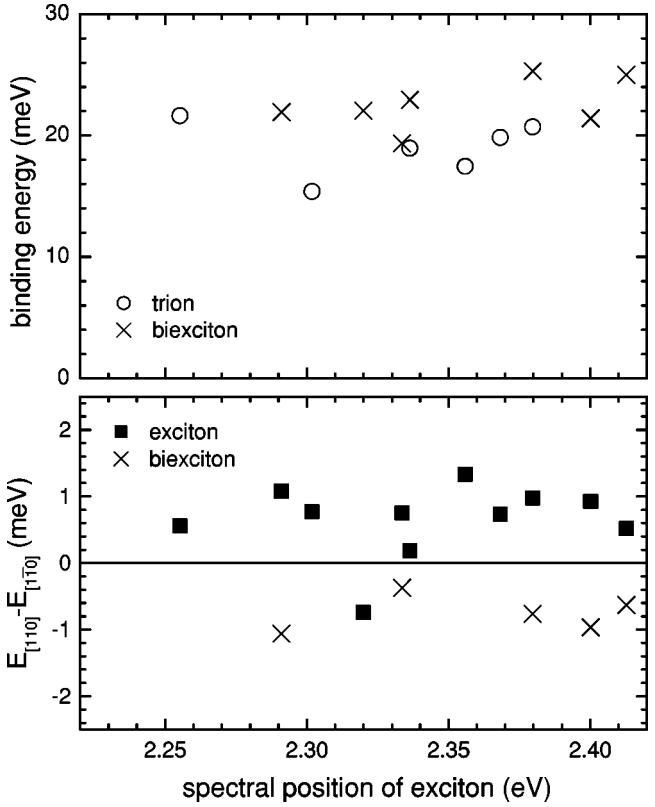

FIG. 3. Top: the binding energy of trions and biexcitons vs the spectral position of the transition. Bottom: the polarization splitting observed for biexcitons and excitons vs the spectral position of the transition.

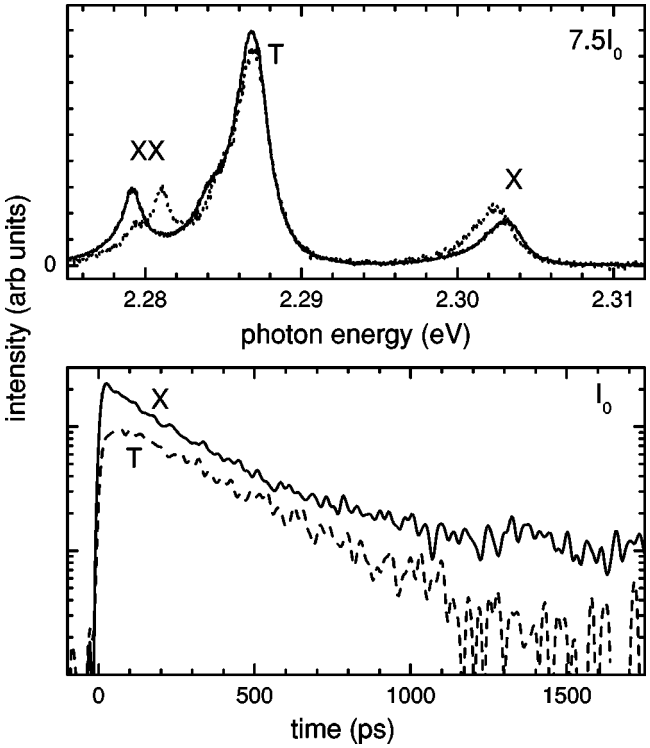

FIG. 4. Top: time-integrated photoluminescence for linear polarizations along [110] (solid line) and $[1\bar{1}0]$ (dashed line). Bottom: time-resolved photoluminescence intensity (logarithmic scale) of the exciton (X) and trion (T) emission after pulsed excitation at time zero. The excitation intensity was $I_0 = 250\ \mu$W.

momentum of $\pm 1\hbar$ and a nonradiative (dark) doublet of $\pm 2\hbar$. In QD's of cylindrical symmetry in (001) direction (point group symmetry D_{2d}) the dark doublet is split further by a splitting energy δ_2. Breaking the cylindical symmetry, e.g., by an anisotropic confinement potential splits the bright doublet by a splitting energy δ_1 into two states which have optical transitions to the ground state which are linearly polarized along the two orthogonal principal axes of the elliptical part of the anisotropy. For single excitons in CdSe/ZnSe QD's values of δ_1 between 0 and more than 0.8 meV were reported.[7] In a CdSe/ZnSe QD ensemble, average values of $\delta_0 = 1.9$ meV, $\delta_1 = 0.2$ meV, and $\delta_2 < 0.02$ meV (Ref. 56) were measured. For comparison, in CdTe/ZnTe quantum dots bright-state splittings δ_1 from 0.06 to 0.32 meV were found.[25]

The observed polarization splittings $E_{[110]} - E_{[1\bar{1}0]} = \delta_1$ of the exciton peak plotted in Fig. 3 are thus an indication of anisotropically confined excitons. The asymmetry-induced splitting does not show a systematic size dependence, similar to findings in InGaAs QD's.[37] However, the splitting has dominantly a positive sign for the exciton, so that the exciton anisotropy is not random, but its size is preferentially larger in the $[1\bar{1}0]$ crystal direction.[57]

The consequences of the exchange interaction for the fine structure of the biexciton and trion transitions are the following: The trion ground state is a spin-singlet state and the wave function overlap of the two electrons (or holes) in the trion gives zero local spin density of the two electron (holes). The remaining third carrier does not experience an exchange interaction and thus the trion peak does not exhibit an exchange splitting. To within the experimental resolution (100 μeV) we have not observed any trion polarization splitting. Because the biexciton has no spin degeneracy, the biexciton to exciton transition shows the (inverted) fine structure of the exciton transition.[7,58] Therefore the peak positions of the linearly polarized exciton and biexciton transitions are inverted relative to each other, in agreement with our experiment (see, e.g., Fig. 4, upper panel). The polarization splitting observed for the biexciton is 0.2–1.2 meV as can be seen in Fig. 3. As expected, the observed exchange splitting of the exciton and biexciton is, within the experimental accuracy equal. We have not seen any relationship between the magnitude of the polarization splitting and other parameters such as the biexciton binding energy or the transition energy.

B. Decay dynamics

Having assigned the transitions within our spectra, we now turn to an analysis of the time-resolved emission from the dots. Figure 4 shows the time-resolved decay of a trion and an exciton at a low excitation intensity along with the corresponding time-integrated photoluminescence spectrum for this dot. We have fitted the data for the exciton with a bicomponent exponential decay (Fig. 4, lower panel). The

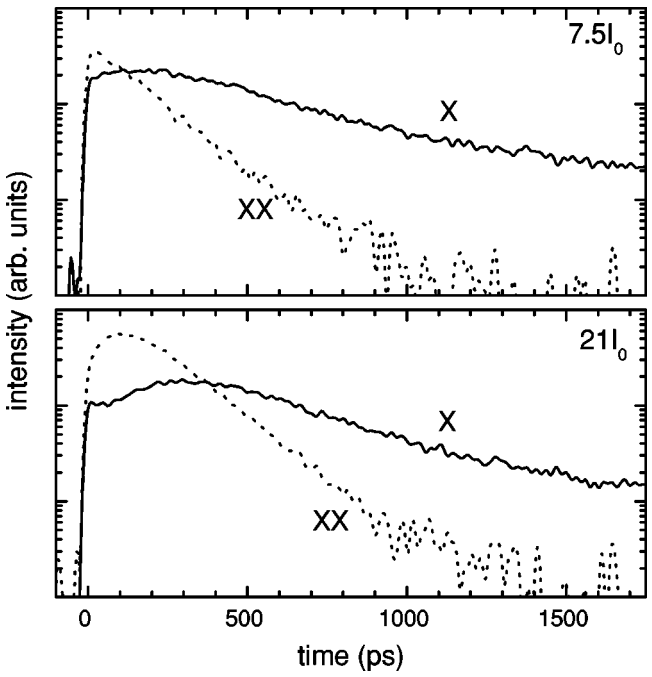

FIG. 5. Top: time-resolved photoluminescence plot of an exciton (X) and biexciton (XX) for the same quantum dot. Bottom: the same features as above at a higher excitation intensity such that the biexciton also shows signs of refilling.

initial decay is dominated by a part with a decay constant of 240 ps. The second component of the decay has a decay constant of 2.5 ± 0.5 ns. We attribute this long-time component to a repopulation process of the bright- from the dark-exciton states. From the presence of the long-time component it is clear that there is a finite probability of a transition between bright- and dark-exciton states, which presents an additional channel for the initial population decay of the bright-exciton state. The initial decay time of 240 ps is thus not purely due to radiative decay. Note that the trion does not possess such a dark ground state and, indeed, we see it exhibit no such behavior at long times. Instead we observe a single exponential decay with a time of 320 ps. In addition, it shows an initial refilling behavior, which is not shown by the exciton, even at low excitation intensities. We attribute this to a spin-relaxation process in which the trion starts from a state with equal spin for all carriers, which is a dark state. One of the two equal carriers is in the first excited electronic state since Pauli blocking prevents the relaxation into the ground state. A spin flip lifts the blocking and allows the carrier to relax. After the spin flip, the trion state is bright and the radiative recombination can be observed. The probability of creating the discussed initial state by nonresonant optical pumping, assuming a random spin distribution of the carriers, is only 1/4, so that the slow process does not dominate the average trion emission dynamics. The observed rise has a time constant of 30–50 ps, which we attribute to the discussed spin-flip relaxation.

Figure 5 shows the time-resolved photoluminescence of the exciton and biexciton transition for medium and high excitation intensities. The biexciton is fitted by a monoexponential decay and was found to have a decay time of 170 ps

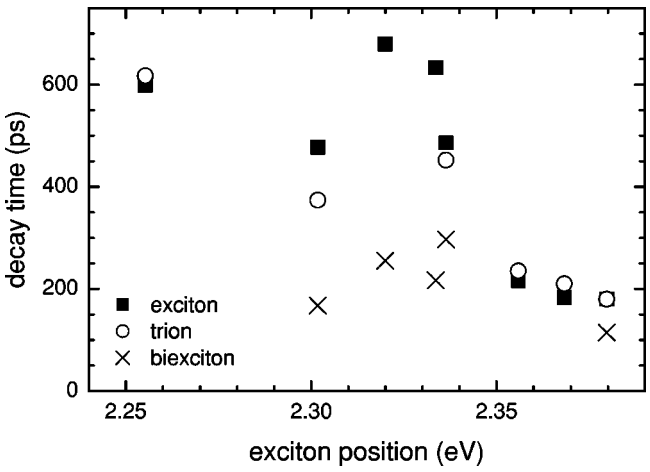

FIG. 6. Measured PL intensity decay times for exciton, biexciton, and trion transitions in multiple quantum dots vs the corresponding exciton transition energy.

which is faster than the exciton. In most cases we found that the ratio of the exciton decay time to the biexciton decay time was approximately 2:1, in contrast to some previous results[8] but in agreement with ensemble data[5] and recent experiments on InAs quantum dots[59] which also show an enhancement of the biexciton decay rate over that of the exciton. For both intensities shown in Fig. 5 the exciton now shows an initial refilling. A good fit is obtained by setting the time constant for this refilling to the decay time of the biexciton. At the highest intensities we also see evidence for refilling of the biexciton from states which have three or more excitons in the dot. Examination of the spectra from the streak camera at times soon after the excitation of the sample showed a short-lived peak 4 meV below the biexciton. Its decay time of 140 ps is comparable to the rise time of the biexciton at this intensity and so we have tentatively labeled it as a triexciton. Naturally, further examination of the properties of this peak would be required to make this identification more trustworthy. We have seen that also the trion, which does not show refilling at medium excitation intensity, at the highest excitation intensities begins to show refilling as well, with a time constant comparable to that of the biexciton decay. While this does suggest that a charged biexciton is responsible for this effect, we have been unable to isolate a peak corresponding to this transition and so also cannot present an energy splitting.

Beside this representative quantum dot discussed in Figs. 4 and 5, we screened the decay dynamics of a much larger number of quantum dots. Figure 6 shows the resulting decay times for the different transitions in the investigated single-dot ensemble.[60] In general, we find that the trion has a lifetime comparable to that of the exciton, while the biexciton has a lifetime which is shorter than the exciton, typically by a factor of 2. The result for the ratio of the exciton:biexciton lifetime of 2:1 is in agreement with earlier data measured at ensembles[5] and recent single-dot experiments.[59]

The observed systematic increase of the decay times with decreasing transition energy (see Fig. 6) is in agreement with measurements on the ensemble[5] and is attributed to the de-

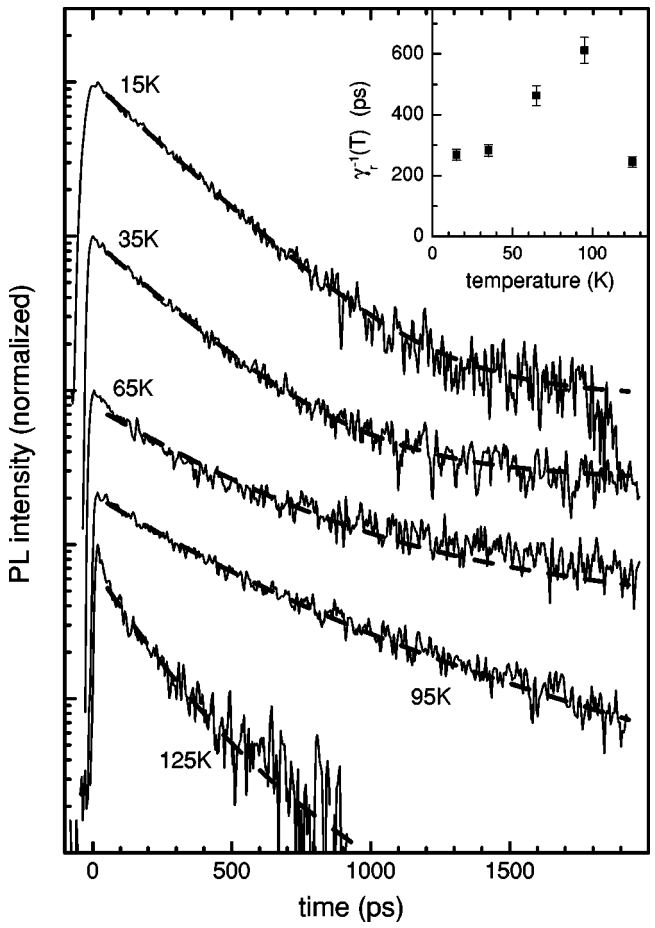

FIG. 7. Time-resolved photoluminescence decay of the exciton at varying temperatures as indicated. The inset shows the extracted temperature dependence of the effective radiative lifetime $\gamma_r^{-1}(T)$ of the spin-singlet exciton state ensemble (see text).

creasing coherence volume of the excitons with increasing localization. While trions and biexcitons are characterized by an almost monoexponential decay, the presence of a dark state complicates the analysis of the exciton dynamics.

The interplay between the lowest forbidden and higher allowed exciton states becomes even more clear in the temperature dependence of the exciton dynamics. Thermally activated repopulation of the bright-exciton state from the energetically lowest dark exciton has been already reported for CdSe nanocrystals[61]; however, the analysis in the decay dynamics was limited to the nanosecond time range given by the time resolution of the used single-photon counting system. In the next section we therefore give an overview of the temperature-induced change in the exciton dynamics in the early time range <2 ns using data from a streak camera.

C. Temperature dependence of emission

In Fig. 7 we show the emission of an exciton transition for varying temperatures and at low excitation intensities, at which the biexciton emission is negligible. It can be seen that at the lowest temperatures the emission dynamics is dominated by the decay of the exciton and, compared to higher temperatures, repopulation from the dark state is suppressed. With increasing temperature the repopulation of the exciton from the dark state is seen to increase so that by 65 K the emission dynamics contain a strong contribution from the dark-state refilling. Above 100 K there is a strong decrease in the lifetime of all transitions, presumably due to the thermal escape of the carriers out of the dots and subsequent nonradiative recombination.

To analyze the measured PL transients, we apply a simple rate equation model. At low temperatures, the dynamics after the initial relaxation is dominated by the radiative decay γ_r and the phonon-assisted scattering quantified by the rate γ_0 between the two bright- (spin-singlet) and the two dark- (spin-triplet) exciton states. The dark-state energy is by δ_0 lower than the bright-state energy. At higher temperatures, both the thermal population of excited exciton states and the thermal escape into the ZnCdSe QW states have to be included. The thermal population of excited exciton states is a fast process relative to escape and spin flip, so that we can take it into account by considering a temperature-dependent effective radiative decay rate $\gamma_r(T)$ of the spin-singlet exciton states. The escape is modeled by a phonon-assisted transition with a given escape energy δ_e and a scattering rate γ_e. The recapture into the dot is assumed to be negligible, since in the small mesa structures under investigation the carriers are mostly captured into surface states. This is supported by the thermally activated decrease of the time-integrated emission intensity. With these assumptions, the rate equations for the probability of bright excitons (n_b) and dark excitons (n_d) can be written as

$$\partial_t n_b = -n_b(\gamma_r + (1+N_0)\gamma_0 + N_e\gamma_e) + n_d N_0 \gamma_0,$$

$$\partial_t n_d = -n_d(N_0\gamma_0 + N_e\gamma_e) + n_b(1+N_0)\gamma_0. \qquad (4)$$

$N_{0,e}$ denotes the Bose occupation number of phonons $[\exp(\delta_{0,e}/k_B T)-1]^{-1}$ at the energies $\delta_{0,e}$ of bright-dark splitting and escape, respectively. Since the PL is excited nonresonantly with linear polarization, the carriers lose their spin polarization during the phonon-assisted relaxation into the dots, and we can assume an initially equal probability of creating bright or dark excitons—i.e., $n_b(0)=n_d(0)$. Since the excited average exciton number is less than 1, the effect of multiexciton states on the dynamics[62] is not considered.

The set of temperature-dependent transients of the PL intensity can be fitted with the analytical solution of Eqs. (4) for $n_b(t)$, since the intensity is proportional to the probability of the exciton being in the bright state. A consistent fit (see dashed lines in Fig. 7) is found for the parameters $\delta_0 = 1.5$ meV, $\delta_e = 30$ meV, $\gamma_0 = 0.08$ ns^{-1}, $\gamma_e = 30$ ns^{-1}, and the temperature-dependent effective radiative lifetime of the spin-singlet states $\gamma_r^{-1}(T)$ shown in the inset. The value of δ_0 is similar to previous findings,[56] and the escape energy δ_e is close to the LO-phonon energy of ZnSe (31 meV), indicating that the escape is proceeding via LO-phonon absorption. The spin relaxation time γ_0^{-1} is about 13 ns, much longer than the radiative decay rate. This is consistent with previous observations of the bright-state spin dynamics.[20] The radiative lifetime γ_r^{-1} is 270 ps at low temperature, where only the lowest electronic states are populated. With

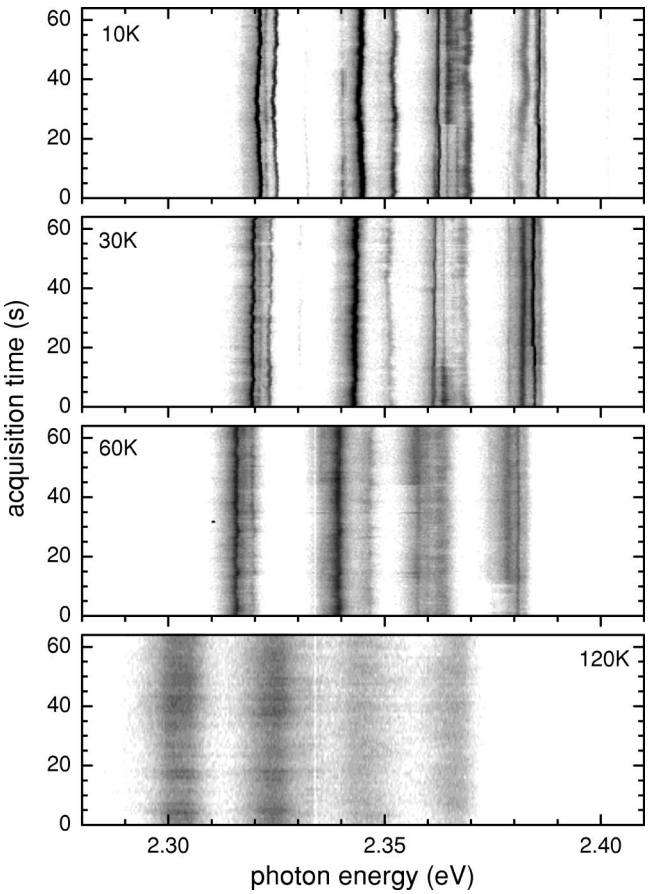

FIG. 8. Spectrally resolved intensity vs time (logarithmic greyscale) shown at temperatures of (from top) 10, 30, 60, and 120 K.

increasing temperature, the effective $\gamma_r^{-1}(T)$ of the spin-singlet exciton states is increasing due to the population of excited exciton states, of which a large fraction has smaller radiative rates due to the small envelope function overlap between electron and hole.

The long-time dynamics (spectral wandering) also changes with temperature, as shown in Fig. 8. This dynamics can be divided into a continuous jitter of the spectral position and intensity of spectral features, and of abrupt changes of the spectral intensity. With increasing temperature, the homogeneous linewidth of the emission increases, so that the spectral jitter becomes less obvious. The low-frequency components of the spectral jitter decrease with increasing temperature, so that at 120 K only fast intensity jitter is remaining. We leave our discussion at this qualitative level, while a quantitative analysis and modeling like in Refs. 23,24,36,63 and 64 is not attempted.

IV. SUMMARY

We have analyzed the nonresonantly excited photoluminescence of samples containing few CdSe/ZnSe quantum dots. By using the dynamic shift in the spectral position of emission peaks we were able to correlate these peaks and hence identify transitions within single dots to excitons, trions, and biexcitons. Analysis of both polarization and time-resolved data allowed us to identify the quasiparticles responsible for these peaks and subsequently present data on their dynamics.

The trions have a binding energy of 15–22 meV, only slightly smaller than the biexciton binding energy of 19–26 meV. In the same dot, the biexciton binding was always some meV higher that the trion binding energy. The exchange splitting of the two bright-single-exciton states was found to be in the range of 1 meV and preferentially oriented along one crystal axis ($[110]$ or $[1\bar{1}0]$).

The population dynamics was measured by time-resolved photoluminescence. In general, we find that the trion has a lifetime comparable to that of the exciton, while the biexciton has a lifetime which is shorter than the exciton, typically by a factor of 2. A systematic increase of the decay times with decreasing transition energy is found. The trion dynamics shows a refilling from an excited trion state that decays radiatively only after phonon-assisted spin and energy relaxation with a time constant of several tens of picoseconds. The exciton dynamics shows a refilling from the dark state for long times, which was modeled by a temperature-dependent rate equation. The deduced spin relaxation time between singlet and triplet exciton states at low temperatures is 13 ns.

ACKNOWLEDGMENTS

The authors are grateful to K. Leonardi and D. Hommel from the University Bremen for growing the samples and T. Kümmell and A. Forchel from the University Würzburg for etching the mesa structures.

*Electronic address: woggon@fred.physik.uni-dortmund.de

[1] N.N. Ledentsov, I.L. Krestnikov, M.V. Maximov, S.V. Ivanov, S.L. Sorokin, P.S. Kopev, Zh.I. Alferov, D. Bimberg, and C.M. Sotomayor-Torres, Appl. Phys. Lett. **69**, 1343 (1996).

[2] U. Woggon, W. Petri, A. Dinger, S. Petillon, M. Hetterich, M. Grün, K.P. O'Donnell, H. Kalt, and C. Klingshirn, Phys. Rev. B **55**, 1364 (1997).

[3] M. Strassburg, V. Kutzer, U.W. Pohl, A. Hoffmann, I. Broser, N.N. Ledentsov, D. Bimberg, A. Rosenauer, U. Fischer, and D. Gerthsen, Appl. Phys. Lett. **72**, 942 (1998).

[4] S.V. Ivanov, A.A. Toropov, S.V. Sorokin, T.V. Shubina, I.V. Sedova, A.A. Sitnikova, P.S. Kopev, Zh.I. Alferov, H.-J. Lugauer, G. Reuscher, M. Keim, F. Fischer, A. Waag, and G. Landwehr, Appl. Phys. Lett. **74**, 498 (1999).

[5] F. Gindele, U. Woggon, W. Langbein, J.M. Hvam, K. Leonardi, D. Hommel, and H. Selke, Phys. Rev. B **60**, 8773 (1999).

[6] F. Gindele, K. Hild, W. Langbein, and U. Woggon, Phys. Rev. B **60**, R2157 (1999).

[7] V.D. Kulakovskii, G. Bacher, R. Weigand, T. Kümmell, A. Forchel, E. Borovitskaya, K. Leonardi, and D. Hommel, Phys. Rev. Lett. **82**, 1780 (1999).

[8] G. Bacher, R. Weigand, J. Seufert, V.D. Kulakovskii, N.A. Gippius, A. Forchel, K. Leonardi, and D. Hommel, Phys. Rev. Lett. **83**, 4417 (1999).

[9] U. Woggon, K. Hild, F. Gindele, W. Langbein, M. Hetterich, M. Grün, and C. Klingshirn, Phys. Rev. B **61**, 12 632 (2000).
[10] S.H. Xin, P.D. Wang, Aie Yin, C. Kim, M. Dobrowolska, J.L. Merz, and J.K. Furdyna, Appl. Phys. Lett. **69**, 3884 (1996).
[11] Y.H. Wu, K. Arai, and T. Yao, Phys. Rev. B **53**, R10 485 (1996).
[12] Hyun-Chui Ko, Doo-Cheol Park, Y. Kawakami, S. Fujita, and S. Fujita, Appl. Phys. Lett. **70**, 3278 (1997).
[13] K. Leonardi, H. Heinke, K. Ohkawa, D. Hommel, H. Selke, F. Gindele, and U. Woggon, Appl. Phys. Lett. **71**, 1510 (1997); F. Gindele, C. Märkle, U. Woggon, W. Langbein, J.M. Hvam, K. Leonardi, K. Ohkawa, and D. Hommel, J. Cryst. Growth **184/185**, 306 (1998).
[14] D. Schikora, S. Schwedhelm, D.J. As, K. Lischka, D. Litvinov, A. Rosenauer, D. Gerthsen, M. Strassburg, A. Hoffmann, and D. Bimberg, Appl. Phys. Lett. **76**, 418 (2000).
[15] F. Flack, N. Samarth, V. Nikitin, P.A. Crowell, J. Shi, J. Levy, and D.D. Awschalom, Phys. Rev. B **54**, R17 312 (1996).
[16] M. Lowisch, M. Rabe, B. Stegemann, F. Henneberger, M. Grundmann, V. Türck, and D. Bimberg, Phys. Rev. B **54**, R11 074 (1996).
[17] M. Rabe, M. Lowisch, and F. Henneberger, J. Cryst. Growth **184/185**, 248 (1998); H. Kirmse, R. Schneider, M. Rabe, W. Neumann, and F. Henneberger, Appl. Phys. Lett. **72**, 1329 (1998).
[18] J.C. Kim, H. Rho, L.M. Smith, H.E. Jackson, S. Lee, M. Dobrowolska, and J.K. Furdyna, Appl. Phys. Lett. **75**, 214 (1999).
[19] J. Seufert, M. Rambach, G. Bacher, A. Forchel, M. Keim, S. Ivanov, A. Waag, and G. Landwehr, Phys. Rev. B **62**, 12 609 (2000).
[20] T. Flissikowski, A. Hundt, M. Lowisch, M. Rabe, and F. Henneberger, Phys. Rev. Lett. **86**, 3172 (2001).
[21] S.A. Empedocles, D.J. Norris, and M.G. Bawendi, Phys. Rev. Lett. **77**, 3873 (1996).
[22] B.P. Zhang, Y.Q. Li, T. Yasuda, W.X. Wang, Y. Segawa, K. Edamatsu, and T. Itoh, Appl. Phys. Lett. **73**, 1266 (1998).
[23] J. Seufert, R. Weigand, G. Bacher, T. Kümmell, A. Forchel, K. Leonardi, and D. Hommel, Appl. Phys. Lett. **76**, 1872 (2000); J. Seufert, M. Obert, M. Scheibner, N.A. Gippius, G. Bacher, A. Forchel, T. Passow, K. Leonardi, and D. Hommel, *ibid.* **79**, 1033 (2001).
[24] V. Türck, S. Rodt, O. Stier, R. Heitz, R. Engelhardt, U.W. Pohl, D. Bimberg, and R. Steingrüber, Phys. Rev. B **61**, 9944 (2000).
[25] L. Marsal, L. Besombes, F. Tinjod, K. Kheng, A. Wasiela, B. Gilles, J.-L. Rouviere, and H. Mariette, J. Appl. Phys. **91**, 4936 (2002).
[26] K. Kheng, R.T. Cox, Merle Y. dÁubigne, F. Bassani, K. Saminadayar, and S. Tatarenko, Phys. Rev. Lett. **71**, 1752 (1993).
[27] G. Finkelstein, H. Shtrikman, and I. Bar-Joseph, Phys. Rev. Lett. **74**, 976 (1995).
[28] A.J. Shields, M. Pepper, M.Y. Simmons, and D.A. Ritchie, Phys. Rev. B **52**, 7841 (1995).
[29] E. Vanelle, M. Paillard, X. Marie, T. Amand, P. Gilliot, D. Brinkmann, R. Levy, J. Cibert, and S. Tatarenko, Phys. Rev. B **62**, 2696 (2000).
[30] A. Esser, E. Runge, R. Zimmermann, and W. Langbein, Phys. Rev. B **62**, 8232 (2000).
[31] G.V. Astakhov, D.R. Yakovlev, V.P. Kochereshko, W. Ossau, W. Faschinger, J. Puls, F. Henneberger, S.A. Crooker, Q. McCulloch, D. Wolverson, N.A. Gippius, and A. Waag, Phys. Rev. B **65**, 165335 (2002)
[32] T. Taliercio, P. Lefebvre, V. Calvo, D. Scalbert, N. Magnea, H. Mathieu, and J. Allegre, Phys. Rev. B **58**, 15 408 (1998).
[33] J.J. Finley, A.D. Ashmore, A. Lemaitre, D.J. Mowbray, M.S. Skolnick, I.E. Itskevich, P.A. Maksym, M. Hopkinson, and T.F. Krauss, Phys. Rev. B **63**, 073307 (2001).
[34] V. Türck, S. Rodt, R. Heitz, O. Stier, M. Strassburg, U.W. Pohl, and D. Bimberg, Phys. Status Solidi B **224**, 217 (2001).
[35] K. Hild, D. Miller, W. Langbein, U. Woggon, M. Hetterich, and C. Klingshirn, Phys. Status Solidi B **224**, 379 (2001).
[36] L. Besombes, K. Kheng, L. Marsal, and H. Mariette, Phys. Rev. B **65**, 121314(R) (2002).
[37] M. Bayer, G. Ortner, O. Stern, A. Kuther, A.A. Gorbunov, A. Forchel, P. Hawrylak, S. Fafard, K. Hinzer, T.L. Reinecke, S.N. Walck, J.P. Reithmaier, F. Klopf, and F. Schäfer, Phys. Rev. B **65**, 195315 (2002).
[38] J.G. Tischler, A.S. Bracker, D. Gammon, and D. Park, Phys. Rev. B **66**, 081310(R) (2002).
[39] I.A. Akimov, A. Hundt, T. Flissikowski, and F. Henneberger, Appl. Phys. Lett. **81**, 4730 (2002).
[40] K.T. Shimizu, W.K. Woo, B.R. Fisher, H.J. Eisler, and M.G. Bawendi, Phys. Rev. Lett. **89**, 117401 (2002).
[41] A. Franceschetti and A. Zunger, Phys. Rev. B **62**, R16 287 (2000).
[42] J. Shumway, A. Franceschetti, and A. Zunger, Phys. Rev. B **63**, 155316 (2001).
[43] A. Wojs and P. Hawrylak, Phys. Rev. B **55**, 13 066 (1997).
[44] Al.L. Efros and A.V. Rodina, Solid State Commun. **72**, 645 (1989).
[45] M. Illing, G. Bacher, T. Kümmell, A. Forchel, T.G. Andersson, D. Hommel, B. Jobst, and G. Landwehr, Appl. Phys. Lett. **67**, 124 (1995).
[46] The biexciton binding energy is derived by calculating the energy difference with respect to the energy of the bright exciton; i.e., we neglect the correction due to polarization splitting introduced in Ref. 7. Since the observed polarization splitting is smaller than the experimentally obtained standard deviation of the biexciton binding energy itself, this approximation is justified.
[47] Al.L. Efros, M. Rosen, M. Kuno, M. Nirmal, D.J. Norris, and M. Bawendi, Phys. Rev. B **54**, 4843 (1996).
[48] A. Franceschetti, L. Wang, H. Fu, and A. Zunger, Phys. Rev. B **58**, R13 367 (1998).
[49] E.L. Ivchenko and G. Pikus, *Superlattices and other Heterostructures* (Springer-Verlag, Berlin, 1995).
[50] S.V. Goupalov and E.L. Ivchenko, J. Cryst. Growth **184/185**, 393 (1998).
[51] M. Nirmal, D.J. Norris, M. Kuno, M.G. Bawendi, A.L. Efros, and M. Rosen, Phys. Rev. Lett. **75**, 3728 (1995).
[52] M. Chamarro, C. Gourdon, P. Lavallard, O. Lublinskaya, and A.I. Ekimov, Phys. Rev. B **53**, 1336 (1996).
[53] U. Woggon, F. Gindele, O. Wind, and C. Klingshirn, Phys. Rev. B **54**, 1506 (1996).
[54] D. Gammon, E.S. Snow, B.V. Shanabrook, D.S. Katzer, and D. Park, Phys. Rev. Lett. **76**, 3005 (1996).
[55] F. Gindele, U. Woggon, W. Langbein, J.M. Hvam, M. Hetterich, and C. Klingshirn, Solid State Commun. **106**, 653 (1998).
[56] J. Puls, M. Rabe, H.J. Wünsche, and F. Henneberger, Phys. Rev. B **60**, R16 303 (1999).
[57] We could only determine the orthogonal directions [110] and $[1\bar{1}0]$ by the orthogonal cleavage facets of the crystal. This leaves an ambiguity in the ordering. Since all QD's are on the

same crystal, their relative polarization orientation is unambiguous.

[58] L. Besombes, K. Kheng, and D. Martrou, Phys. Rev. Lett. **85**, 425 (2000).

[59] C. Santori, G.S. Solomon, M. Pelton, and Y. Yamamoto, Phys. Rev. B **65**, 073310 (2002).

[60] Note that the times given in Fig. 6 in the case of the exciton are for the fast initial decay.

[61] X. Fan, M.C. Lonergan, Y. Zhang, and H. Wang, Phys. Rev. B **64**, 115310 (2001).

[62] M. Ikezawa and Y. Masumoto, Phys. Rev. B **53**, 13 694 (1996).

[63] R.G. Neuhauser, K.T. Shimizu, W.K. Woo, S.A. Empedocles, and M.G. Bawendi, Phys. Rev. Lett. **85**, 3301 (2000).

[64] K.T. Shimizu, R.G. Neuhauser, C.A. Leatherdale, S.A. Empedocles, W.K. Woo, and M.G. Bawendi, Phys. Rev. B **63**, 205316 (2001).